Toward a Single-electron Image Processor for Edge Detection based on the Inner Retina Model

Andrew Kilinga Kikombo†*, Alexandre Schmid‡, Tetsuya Asai†, Yusuf Leblebici‡ and Yoshihito Amemiya†

†Grad. Sch. of Information Science & Technology, Hokkaido Univ.
Kita 14, Nishi9, Kita-ku, Sapporo, 060-0814 Japan.
Phone:+81-11-706-7147, Fax:+81-11-706-7890
∗ email: kikombo@sapiens-ei.eng.hokudai.ac.jp

‡Microelectronic Systems Laboratory,
Swiss Federal Institute of Technology (EPFL)
Lausanne, CH-1015 Switzerland.

Abstract

We propose a possible circuit structure consisting of single-electron circuits that performs edge extraction and enhancement in projected images. Electrical circuits that are designed by mimicking computational structures in living organisms—*neuromorphic* LSI circuits, would provide an insight in developing even more efficient processors. In this work, based on a well studied model for edge detection in the vertebrate retina, we propose a single-electron circuit performing the same function, and demonstrate its operation with a one- and a two-dimensional array circuit.

1. Introduction

In the past decades, miniaturization of transistors has been the basic method to realize more efficient information processors. However, due to scaling limitations facing further miniaturization, several novel approaches to achieve enhanced processor performances are being considered as alternatives. These include novel architectural approaches, for instance, information processors based on how living organisms carry out information processing—*neuromorphic* engineering [1]. Neuromorphic circuit architectures would provide a breakthrough to creating highly parallel, real-time information processors. So far, a number of neuromorphic LSIs suitable for implementation only with CMOS mediums have been proposed.

In this paper, based on a well studied model for edge detection in the vertebrate retina ([2] - [4]), we propose a possible architecture for an image processor consisting of single-electron devices. Edge detection is a primary function in early stage visual processing carried out in the vertebrate retina. The proposed structure carries out edge detection in projected images.

We start by giving details on the retinal model for edge detection, then illustrate how to realise constitutive elements in the model. We then show the circuit configuration of a unit pixel. We finally demonstrate the performance of the proposed processor through Monte-Carlo based computer simulations.

2. Model

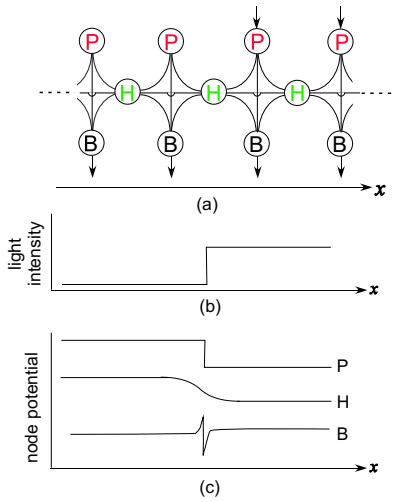

Figure 1: Cross section of the vertebrate retina, showing neurons involved in edge detection; (a) Model: P—Photoreceptors, H—Horizontal cells, B—Bipolar cells. (b) Intensity profile of incident light (c) Potentials of P, H, and B cells, showing response to incident light input.

The vertebrate retina consists of massively interconnected neural cells in a hierarchical structure, where edge detection is carried out mainly through three types of cells: (i) photoreceptors which transduce light inputs into electrical signals, (ii) horizontal cells which receive inputs from the superjacent layer of photoreceptors to produce spatially-averaged outputs in relation to the inputs, and (iii) bipolar cells that produce the difference in amplitudes between the outputs of photoreceptors and horizontal cells. The schematic model is shown in Fig. 1(a) . In this model, we assume that illuminated (or non-illuminated) photoreceptors produce low (or high) potentials (Figs. 1(b) and (c)-P). The outputs are spatially averaged by horizontal cells (Fig. 1(c)-H). The bipolar cells detect the position of edges in the incident images by producing the difference in amplitudes between photoreceptors and horizontal cells. This is obtained by subtracting " H "- from their corresponding" P "-values in bipolar cells. Therefore, the non-zero outputs of bipolar cells represent positions of edges in the input image (Fig. 1(c)-B).

3. Circuit implementation

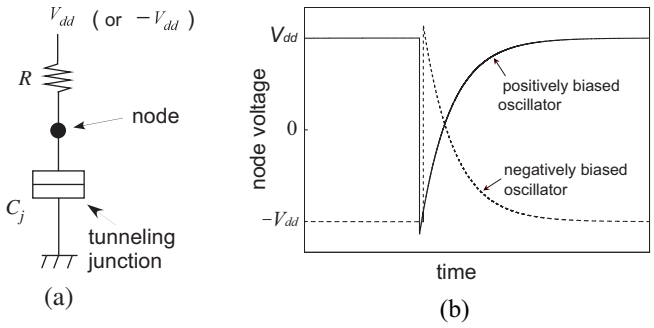

Figure 2: Single electron oscillator; (a) circuit configuration (b) monostable, or one-shot operation of positively biased (solid curve) and negatively biased (dashed curve) oscillators.

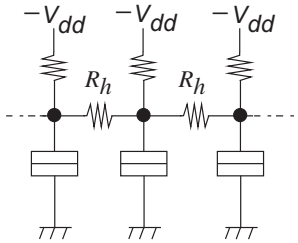

Figure 3: Configuration of the horizontal cell layer.

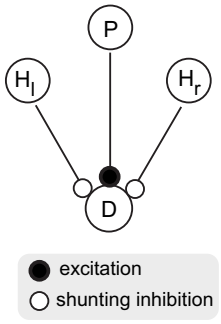

Figure 4: Conceptual configuration of bipolar cells.

Based on the retinal model in the preceding section, we propose a neuromorphic architecture with single-electron oscillators. A single-electron oscillator ([5]) consists of a tunneling junction C_j connected in series to a high resistance R at a node (•) and biased to a voltage source (Fig. 2(a)). It operates as a relaxation oscillator at low temperatures at which the Coulomb-blockade effect takes place. The oscillator is astable if the bias voltage $|V_{dd}| > e/(2C_j)$ (e is the elementary charge) and monostable if $|V_{dd}| < e/(2C_j)$ (see [6] - [7] for detailed explanation). In the absence of external (thermal or trigger input) interference, the node voltage of the monostable oscillator takes the same value with its bias voltage, and retains this equilibrium state. Upon application of an external trigger signal, such as incidence of photons, the Coulomb-blockade is broken off, and electron tunneling occurs through the tunneling junction. The node voltage of a positively biased oscillator drops by e/C_j, because of tunneling from the ground to the node, then gradually increases to return to V_{dd} as junction capacitance C_j is charged through resistance R (Fig. 2(b)-solid curve). In a negatively biased oscillator, the node voltage jumps by e/C_j because of tunneling from the node to the ground, and then gradually decreases to return to $-V_{dd}$ (Fig. 2(b)-dashed curve). To implement photoreceptors, horizontal cells and bipolar cells, we use monostable single-electron oscillators as illustrated below.

3.1. Photoreceptor circuit

Photoreceptors convert light inputs into electrical signals. To realize a photoreceptor, we use a positively biased monostable oscillator. As explained previously, in the absence of external interference, the node voltage is equal to the bias voltage. When a photon is illuminated on a stable oscillator, *photo-induced tunneling effect* ([8] - [9]) occurs inducing electron tunneling from the ground to the nanodot. This leads to a change in the node voltage of the corresponding oscillator from a high to a low value. We refer to this as a firing event. Since light intensity corresponds to the number of photons, high light intensity leads to a high number of tunneling and recharging events, hence a high average firing rate. Therefore positively biased oscillators act as a transducers, converting light inputs into electrical signals.

3.2. Horizontal cell circuit

Horizontal cells receive inputs from the corresponding superjacent photoreceptors to produce a spatially averaged output. To realize the horizontal layer, we need to implement unit horizontal cells and emulate the extensive gap junctions in retinal cells. The horizontal cells are implemented with negatively biased oscillators, while gap junctions are realized through resisitive coupling between neighboring horizontal cells. The construction of the horizontal cell layer is shown in Fig. 3. The photoreceptor cells receive light inputs, inducing electron tunneling from the ground to the node. This leads to a change in node voltage from a positive to a negative value as explained in the previous subsection. The excess charge is transmited to the immediate underlying horizontal cell, acting as an external trigger. At the same time, the excess positive charge from the photoreceptor cell is also transmitted to the other cells in the horizontal layer in such a manner that cells nearest to the tunneling photoreceptor cell would experience a larger decrement in node voltage than those positioned farther. The larger the decrement is, the larger the probability an electron tunneling. Hence the degree of electron tunneling induction in the horizontal cell layer would be inversely proportional to the distance from the tunneling photoreceptor. Thus, the average tunneling rate would decrease with distance from the tunneling cell. Therefore, by resistively coupling neighboring cells in the horizontal layer, we could emulate spatial averaging function of the extensive gap junctions.

3.3. Bipolar cell circuit

Bipolar cells detect the position of edges in incident images by producing the difference in amplitude between corresponding photoreceptor and horizontal cell signals. With conventional CMOS circuits, this could be achieved by using operational amplifiers or through current subtraction method. A similar structure with single-electron devices would require a complicated circuit configuration. Instead of using this conventional approach, we employ neural excitation and shunting inhibition mechanisms to qualitatively imitate subtractive functions in bipolar cells. This mechanism is illustrated in

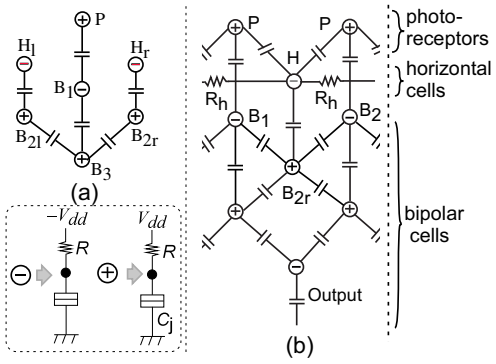

Figure 5: (a) Basic construction of the bipolar cell circuit. (b) Configuration of a unit pixel of the edge detecting circuit consisting of ”P”, ”H”, and ”B” circuit blocks.

Fig. 4. The photoreceptors produce excitatory signals to induce firing in bipolar cells, while the horizontal cells produce inhibitory signals to inhibit the bipolar cells from firing. The average firing rate in the bipolar cells would correspond to the difference between ”P” and ”H” signals.

These two mechanisms are achieved through capacitive couplings between oscillator circuits ([10]-[12]) in the bipolar cell layer. Excitatory coupling is achieved through coupling a negatively biased oscillator to a positively biased one. Electron tunneling, for example in the positively biased oscillator, leads to a decrease in its node voltage. Through the coupling capacitor, this decrease is relayed to the negatively biased oscillator, driving its node voltage far beyond the threshold voltage. This induces electron tunneling in the negatively biased oscillator from the node to the ground—in other words, electron tunneling events are relayed from one oscillator to the other. Shunting inhibition is achieved through coupling oscillators biased to the same voltage. In positively biased oscillators, if tunneling takes place in either of the oscillators, it reduces the node voltage of the other oscillator far below the threshold, thus restraining it from tunneling even in the presence of an external trigger input. By combining these two, we could achieve a basic circuit construction for the bipolar cells (Fig. 5(a)). Excitatory signals are generated along the middle branch P $\rightarrow$ B_1 $\rightarrow$ B_3. P cells receive light inputs to tunnel, consequently inducing tunneling in the negatively biased B_1 cell. B_1 in turn induces tunneling in B_3 as illustrated above. On the other hand, the left and right branches produce an inhibitory signal toward B_3; tunneling in P cells induces tunneling in H_l and H_r cells. These in turn induce tunneling in B_{2l} and B_{2r} respectively. Tunneling in both cells provides a sufficiently large inhibition to restrain B_3 from tunneling, thus blocking signals flowing in the middle branch. This results to a low average tunneling rate in the bipolar cells. Otherwise if tunneling occurs only in either of the two, this won't provide sufficient restraining, leading to a high tunneling rate in the corresponding bipolar cell.

Fig. 5(b) shows a unit pixel of the edge detecting circuit. The photoreceptors receive light inputs to tunnel. This is relayed to the underlying horizontal and bipolar cell layers. The bipolar cells positioned at the edges show a higher tunneling rate in comparison to the other cells. To increase the inhibitory effect of the horizontal cell layer, additional excitatory coupling is introduced between $B_{1,2}$ and B_{2r}.

4. Simulation results

To demonstate the operation of the proposed circuit, we construced a one- and a two-dimensional circuit and confirmed their basic operations through Monte-Carlo based simulations. In the simulations, light input was simulated with an external trigger input of 2.5 mV in amplitude. The gap junction in the horizontal layer was simulated with a resistance R_h = 400 MΩ, excitatory and inhibitory capacitive coupling with a capacitance of 2 aF, tunneling junction capacitance C_j was set to 10 aF, and simulation time was set to 700 ns.

4.1. One-dimensional circuit array

The one-dimensional circuit consists of 100-pixel circuits. Light input was simulated by applying an external trigger input (whose frequency is equivalent to the intensity of light inputs) to corresponding photoreceptors.

The input image was projected between the 33*rd* and the 67*th* photoreceptor. That is, light was evenly illuminated to photoreceptors in this region (with an input trigger of 110 MHz). Fig. 6(a) shows the transient responses of the 50*th* photoreceptor, (b) the 50*th* cell of the subjacent horizontal cell layer and (c), (d) show the response of the 50*th* (middle of the illuminated region) and 33*rd* (left edge) bipolar cell circuits, respectively. The firing rate of bipolar cells within the illuminated region is not zero, however, extremely low compared to the edge cells. The overall response of the ”P”, ”H” and ”B” cells at zero temperature is shown in Fig. 7. The vertical axis is normalised with the maximum firing rate in the photoreceptor layer.

Secondly, we confirmed the response of our circuit to various light intensities. The firing rate of photoreceptors would be proportional to the intensity of input light (section 3.1). This was simulated through altering the frequency of the applied input pulse trigger and computing the average tunneling rates of bipolar cells representing edge positions. The results are shown in Fig. 8. The maximum response frequency was 110 MHz, determined by the minimum charging period within ”P”, ”H”, and ”B” cell layer oscillators.

Thirdly, we evaluated the temperature characteristics. This was carried out to compute the ability to detect edges with increasing temperatures, by deducting the average firing rate of the entire bipolar cell layer from that of edge-position bipolar cells. We refer to this as the SN ratio. Fig. 9 shows the temperature characteristics: (a) edge response simulated at 10 K, (b) SN ratio for temperatures between 0 - 50 K. The vertical axes are normalised with the highest firing rate at zero temperature for (a) and with the SN ratio at zero temperature for (b).

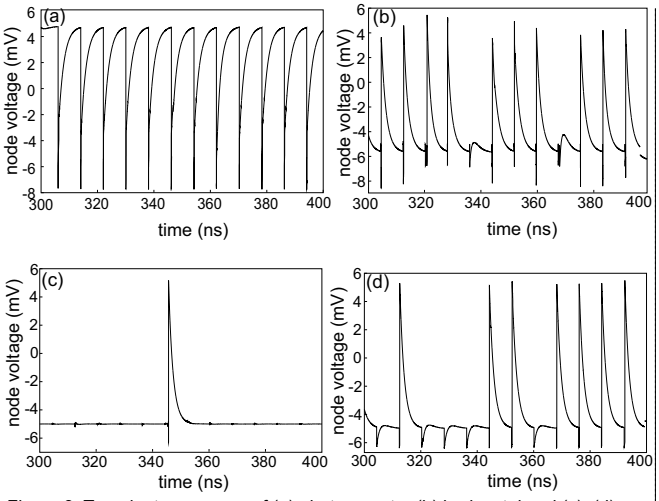

Figure 6: Transient responses of (a) photoreceptor (b) horizontal and (c), (d) bipolar cell circuits: (c) middle of illuminated region, (d) edge cell circuit (T = 0 K).

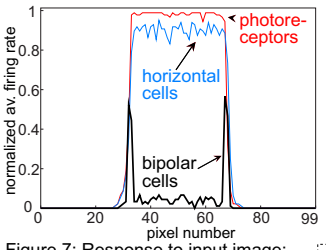

Figure 7: Response to input image: average firing rates of P,H, and B cells

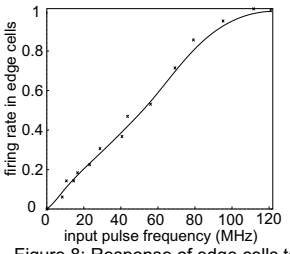

Figure 8: Response of edge cells to light intensity. Simulated at T = 0 K.

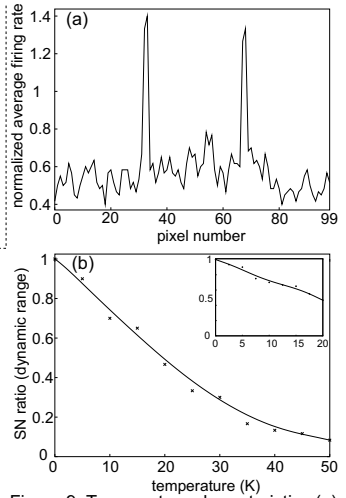

Figure 9: Temperature characteristics (a) Edge detection at T = 10 K, (b) SN ratio (difference between firing rates of edge position cells and entire bipolar cell layer).

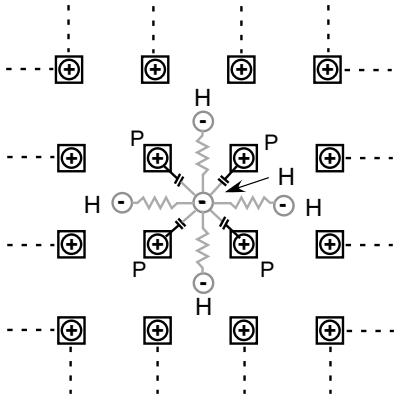

Figure 10: Schematic sketch of the two-dimensional circuit configuration, showing the positions of photoreceptor and horizontal cells.

Figure 11: Edge enhancement results in a gray image: (a) input frame, (b),(c): edge detection results at T = 0 K for (b), and T = 5 K for (c).

4.2. Two-dimensional circuit

The two-dimensional circuit consists of 100×100 pixels. Fig. 10 shows a schematic top view of the circuit. Each cell in the photoreceptor layer is capacitively coupled to 4-horizontal cells in the subjacent horizontal layer. Each of the horizontal cells is resistively coupled to its four adjacent cells in the horizontal layer. Similarly, each of the bipolar cells is capacitively coupled to corrresponding cells in the neigboring 4-pixels. To confirm the operation of the two-dimensional circuit, a gray scale image (Fig. 11(a)) was projected onto the circuit. The simulations results showing edge enhancement in the input image are presented in Fig. 11(b), and (c) for temperature = 0 K, and 5 K respectively.

5. Conclusion

As an inital step to realizing neuromorphic LSI's with single-electron devices, we proposed an edge detecting circuit based on the inner retinal model. Photoreceptors and horizontal cells were implemented with positively- and negatively-biased oscillators respectively. Through neural shunting inhibition and excitation mechanisms, we could achieve the bipolar cells. To confirm the performance of the proposed circuit, we designed a one- and a two-dimensional constructions and evaluated their performances through Monte-Carlo based simulations.

References

[1] R. Douglas, M. Mahowald, and C. Mead, *Annual Review of Neuroscience*, vol. 18, pp. 255-281, 1995.

[2] C. Mead, *Analog VLSI and neural systems*. Addison Wesley, 1989.

[3] A. Moini, *Vision Chips*. Kluwer: 1999.

[4] Shih-Chii Liu *et al.*, *Analog VLSI: Circuits and Principles*. Massachusetts: MIT Press, 2002.

[5] H. Gravert and M.H. Devoret, *Single Charge Tunneling—Coulomb Blockade Phenomena in Nanostructures*. New York: Plenum, 1992.

[6] K.K. Likharev and A.B. Zorin , *J. of Low Temp. Phys.*, vol. 59, pp. 347-382, 1985.

[7] D.V. Averin and K.K. Likharev, *J. of Low Temp. Phys.*, vol. 62, pp. 345-373, 1986.

[8] A. Fujiwara *et al.*, *Phys. Rev. Lett.*, vol. 78, pp. 1532-1535, 1997.

[9] R. Nuryadi *et al.*, *Phys. Rev. B*, vol. 73, pp. 45310-45316, 2006.

[10] T. Oya, T. Asai, T. Fukui, and Y. Amemiya, *Int. J. Unconventional Computing*, vol. 1, no. 2, pp. 177-194, 2005.

[11] T. Oya T., A. Schmid, T. Asai, Y. Leblebici, and Y. Amemiya, *IEICE Electronics Express*, 2, no. 3, pp. 76-80, 2005.

[12] T. Oya, T. Asai, R. Kagaya, T. Hirose, and Y. Amemiya, *Chaos, Solitons & Fractals*, vol. 27, no. 4, pp. 887-894, 2006.